Growth and Atomic-Scale Characterizations of Graphene on Multifaceted Textured Pt Foils Prepared by Chemical Vapor Deposition

Teng Gao,[†,§] Shubao Xie,[†,§] Yabo Gao,[†] Mengxi Liu,[†] Yubin Chen,[†] Yanfeng Zhang,[†,‡,*] and Zhongfan Liu[†,*]

[†]Center for Nanochemistry (CNC), Beijing National Laboratory for Molecular Sciences, State Key Laboratory for Structural Chemistry of Unstable and Stable Species, College of Chemistry and Molecular Engineering, Peking University, Beijing 100871, People's Republic of China and, [‡]Department of Materials Science and Engineering, College of Engineering, Peking University, Beijing 100871, People's Republic of China. [§]These authors contributed equally to this work.

ABSTRACT

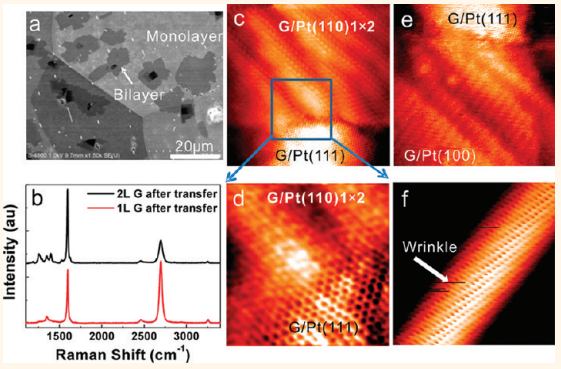

The synthesis of centimeter-scale uniform graphene on Pt foils was accomplished *via* a traditional ambient pressure chemical vapor deposition (CVD) method. Using scanning electron microscopy (SEM) and Raman spectroscopy, we reveal the macroscopic continuity, the thickness, as well as the defect state of as-grown graphene. Of particular importance is that the Pt foils after CVD growth have multifaceted texture, which allows us to explore the substrate crystallography effect on the growth rate and the continuity of graphene. By virtue of atomically resolved scanning tunneling microscopy (STM), we conclude that graphene grows mainly in registry with the symmetries of Pt(111), Pt(110), and Pt(100) facets, leading to hexagonal lattices and striped superstructures. Nevertheless, the carbon lattices on interweaving facets with different identities are connected seamlessly, which ensure the graphene growth from nanometer to micrometer levels. With these results, another prototype for clarifying the preliminary growth mechanism of the CVD process is demonstrated as an analogue of graphene on Cu foils.

KEYWORDS: graphene · STM · chemical vapor deposition (CVD) · growth · Pt foils

Graphene, an ideal two-dimensional material with unique electronic property, has attracted great interest for exploring fundamental questions in condensed matter physics such as quantum Hall effects and for engineering a variety of applications such as transparent electrodes.[1−6] For these targets, preparation of high-quality graphene that is compatible with silicon-based integrated circuits is essential. A major breakthrough on this issue was made by using a simple chemical vapor deposition method (CVD) to synthesize graphene on Cu foils, where predominantly single-layer graphene was achieved possessing the unique traits of low cost, probable for batch production and transferrable to other arbitrary substrates.[7,8]

However, recent reports reveal that the low carrier mobility related with the ever-present grain boundaries will strongly influence the transport property of CVD graphene on Cu foils.[8,9] In this case, studies on the preliminary growth dynamics were advanced, and characterizations of common defects such as domain boundaries and point defects were pursued by obtaining atomic-scale images.[9−13] Besides, seeking other analogue systems as that of graphene on Cu foils was also promoted. Pt and Pt alloys are used widely for hydrogen carbon catalysis. Similar to Cu, the carbon solubility of Pt is nearly 1 order of magnitude lower than that of Ni at the temperature of CVD growth. The relative higher melting temperature (1768 °C) and lower thermal expansion coefficient (8.8 μm m^{-1} K) than that of Cu can reduce surface atom agglomeration and rough morphology at the high temperature of growth, hereby decreasing the density of wrinkles during the thermal quenching process. Meanwhile, theoretical results ensure that Pt introduces minimum effects on the electronic property of graphene because of weak Pt−graphene interactions.[14] Recently, graphene growth on Pt(111) has been commenced inside the ultrahigh vacuum system where Moiré patterns of different periodicities were usually observed to coexist on the

* Address correspondence to yanfengzhang@pku.edu.cn, zfliu@pku.edu.cn.

Received for review September 6, 2011 and accepted October 24, 2011.

Published online October 24, 2011
10.1021/nn203440r

surface.[15] The shortcoming of this method is the necessity of high-cost single-crystal substrates and the limited size of the resulting graphene flakes. Another effort was also made by growing graphene on sputtered thin Pt films.[16]

In this work, we focused on the growth of high-quality graphene on Pt foils *via* a simple ambient pressure CVD method, with the assistance of a variety of characterization methods such as SEM, Raman spectroscopy, and especially scanning tunneling microscopy (STM). The macroscopic morphology, the uniformity of layer thickness, the atomic-scale structure, and the kind of defects on graphene are expected to be revealed. More than this, we also wish to explore the substrate facets on the continuity and the growth rate of graphene at the as-grown state by using atomically resolved STM. Ultimately, the growth mechanism of CVD graphene on Pt foils is expected to be clarified and compared with that of graphene on Cu foils, in the interest of further optimizing the growth parameters, clarifying the potential mechanism of the CVD process, as well as achieving high-quality graphene materials.

RESULTS AND DISCUSSION

In comparison with the low-pressure CVD method, recent reports reveal that the ambient pressure CVD method can be utilized to prepare graphene with the thickness range from submonolayer to few layers on Cu foils by monitoring the carbon source flow rate and the growth time.[17,18] In this research, this CVD method was used for achieving an effective control of graphene thicknesses. Shown in Figure 1a,b are large- and small-scale SEM images of Pt foils after CVD growth. On the basis of the contrast difference in Figure 1a, the surface can be separated into various regions (or so-called grains) with obvious boundaries. In Figure 1b, three grains having the same SEM contrasts are displayed, in which some striped lines with deeper contrast further divide each single grain into several regions mostly presenting near quadrate shapes. The regions probably correspond to different substrate facets with distinctive identities, as reported recently by using SEM and electron back-scattering diffraction (EBSD) analysis, where various facets with different crystalline identities can coexist inside a single grain on Cu foils after CVD growth.[13] However, due to the limitations of our SEM system, the crystallographic facets corresponding to quadrate- and irregular-shape regions cannot be identified. Another interesting feature is the occasionally observed darker striped contrasts emerging at the facet boundaries which can extend to adjacent grains, as exemplified in Figure 1b. They may be wrinkles evolving from the thermal expansion mismatch between graphene and Pt throughout the thermal quenching process of CVD growth. Note that the wrinkles visible by SEM can serve as macroscopic tracers for the formation of continuous graphene.

By increasing the CVD growth time or altering the flow rate of carbon sources, the synthesis of bilayer graphene can be realized, as illustrated by SEM images in Figure 1c,d. The darker patches containing quadrate- and irregular-shaped boundaries are deduced tentatively to be bilayer graphene according to a similar result on Cu foils,[19,20] and these graphene flakes, customarily showing an average size of $\sim$20 μm^2, prefer to reside on the grains with brighter SEM contrasts (Figure 1c,d) which probably belong to the same substrate facets. Sometimes, the flakes can spill over to a neighboring grain and ride on the grain boundaries (Figure 1d,e). This illustrates the capability of graphene spanning over diverse facets with different identities.

At this moment, transferring the graphene sample to other arbitrary substrate is essential for further characterizing the obtained samples. An improved wet chemical etching method is developed with dilute aqua regia as etching solution. An optical microscopy image for the monolayer graphene after transferring onto a 300 nm thick SiO_2 substrate is presented in Figure 1f, where no additional color contrast is observed except for a small portion of the bare SiO_2 substrate locating in the lower right corner. This convinces further the probability to synthesize perfect monolayer graphene, as well as the validity of the used transfer method.

In order to reconfirm the mono- and bilayer nature, Raman spectra for the mono- and bilayer graphene before and after the transfer process are demonstrated in Figure 1g,h, respectively. It is clear to see that similar G and 2D bands as that of exfoliated graphene can be obtained directly on Pt foils in Figure 1g, while the D band with a position of $\sim$1350 cm^{-1} is almost invisible in both spectra. This result differs from the CVD graphene on Cu foils where the pristine spectra can only be acquired by subtracting the strong copper luminescence background.[21] Further analysis shows that the G peaks locate at $\sim$1582 cm^{-1} for both mono- and bilayer samples, with the monolayer peak having an intensity rather weaker than that of the bilayer's. The 2D peaks for both mono- and bilayers lie at $\sim$2700 cm^{-1}, with the bilayer's 2D band having a much wider spectral bandwidth and a more asymmetric shape. Further simulations demonstrate that the 2D band (or peak) for the bilayers can be separated into four sub-bands, in parallel with four permissible transition processes.[22,23] Altogether, the variation trend of G and 2D peaks with graphene thickness agrees well with that of exfoliated graphene on SiO_2, although the intensity for the monolayer sample is much reduced due to the substrate effects. However, after the chemical transfer process, both G and 2D peaks for the monolayer graphene in Figure 1h were dramatically improved in intensity compared to that of the as-grown sample in Figure 1g. The position and the full width at half-maximum (fwhm) of the two peaks were not changed so much with the transfer process. In addition, the Raman

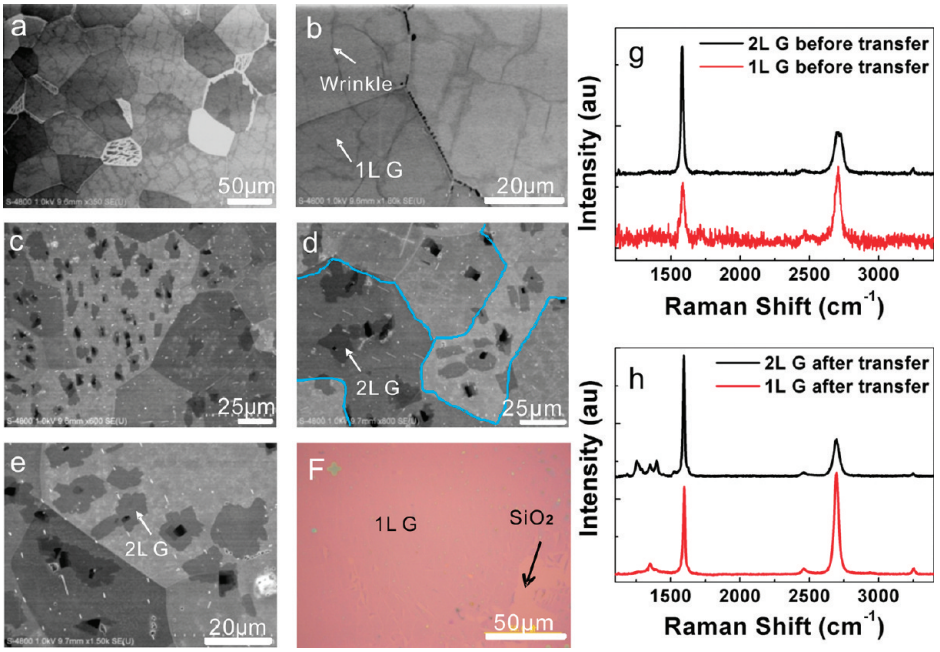

Figure 1. (a) Large-scale SEM image of single-layer graphene growth on Pt foils. (b) Expanded image over three adjacent domains with the same SEM contrasts. The darker stripes in (b) correspond to graphene wrinkles. (c−e) Sequential zoom-in SEM images showing the initial bilayer growth. Bilayer flakes with orthogonal and irregualr boundaries prefer to evlove on Pt domains with brighter SEM contrasts. (f) Optical image of monolayer graphene after transferred onto a 300 nm SiO_2/Si susbtrate. (g,h) Raman spectra of monolayer and bilayer graphene before and after the transfer process, repectively. In panel g, the intensity of the Raman signal for monolayer graphene on Pt foils is magnified by 6 times for a better view.

data for the transferred sample in Figure 1h reflect nearly the same character as that of CVD Cu graphene on SiO_2.[6,7] That means the thickness calibration for the CVD graphene on Pt substrates is reliable.

According to the above data, it can be concluded that the CVD graphene on Pt foils is of high-quality with the thickness controllable from monolayer to bilayer, and the initial bilayer growth preferably occurs on some regions with brighter SEM contrasts, showing tentative clues of substrate crystallographic effects. Moreover, weak interactions between graphene and Pt foils can be deduced by the capability of acquiring Raman spectra on as-grown samples, and this weak interaction was similarly proposed by DFT calculations.[14]

It is noticeable why the growth behaviors of CVD graphene on Pt foils and Cu foils manifest such a consistency. First, note that the physical parameters such as the carbon solubility of both metals is very close and much smaller than that of some transition metals like Ni on which a segregation growth mechanism usually prevails.[24,25] Second, Cu and Pt are perfect catalysts for the decomposition and the dehydrogenation of carbon sources such as methane and ethylene. Accordingly, a surface-mediated or a self-limiting growth mechanism should apply to the monolayer graphene growth on Pt foils. The bilayer growth is proposed to be directed by an epitaxial growth mechanism, as similarly reported on Cu foils.[19]

To obtain the crystallographic feature of Pt foils after CVD growth, the XRD pattern is recorded in Figure 2a, showing dominant (110) facets along with minor (100), (111), and (311) facets. Note that, through increasing sample preannealing time, the latter three facets can be reduced dramatically. Schematic views of these facets are provided in Figure 2b. It is common knowledge that, besides Pt(111), the facet of Pt(110) should be a low energy facet as compared with other high index ones; that is why Pt(110) is the favorite substrate for graphene growth as seen in the XRD data.

It is not so hard to imagine that the multifaceted textured substrates of Pt foils should imply remarkable influence on the atomic-scale structure and the continuity of graphene.[10,12] In the following, intensive investigations were then executed for clarifying this issue. First of all, large-scale STM morphologies are captured in Figure 2c−f, which presents four typical surfaces labeled as case 1, case 2, case 3, and case 4, according to different islands and facets involved. On the basis of the STM height profiles listed below, the four typical surfaces have an average flatness of ~2 nm over a lateral distance of ~400 nm. This surface roughness differs from monolayer graphene growth on polycrystalline Cu and Cu foils, where amorphous and crystalline regions usually coexist with more corrugated surfaces.[12,26] It can be said that the CVD graphene on Pt foils is more flat than that on Cu foils. Even after the chemical etching transfer process, the graphene is expected to possess fewer wrinkles, considering that wrinkles usually evolve on the highly corrugated substrates at the as-grown states.

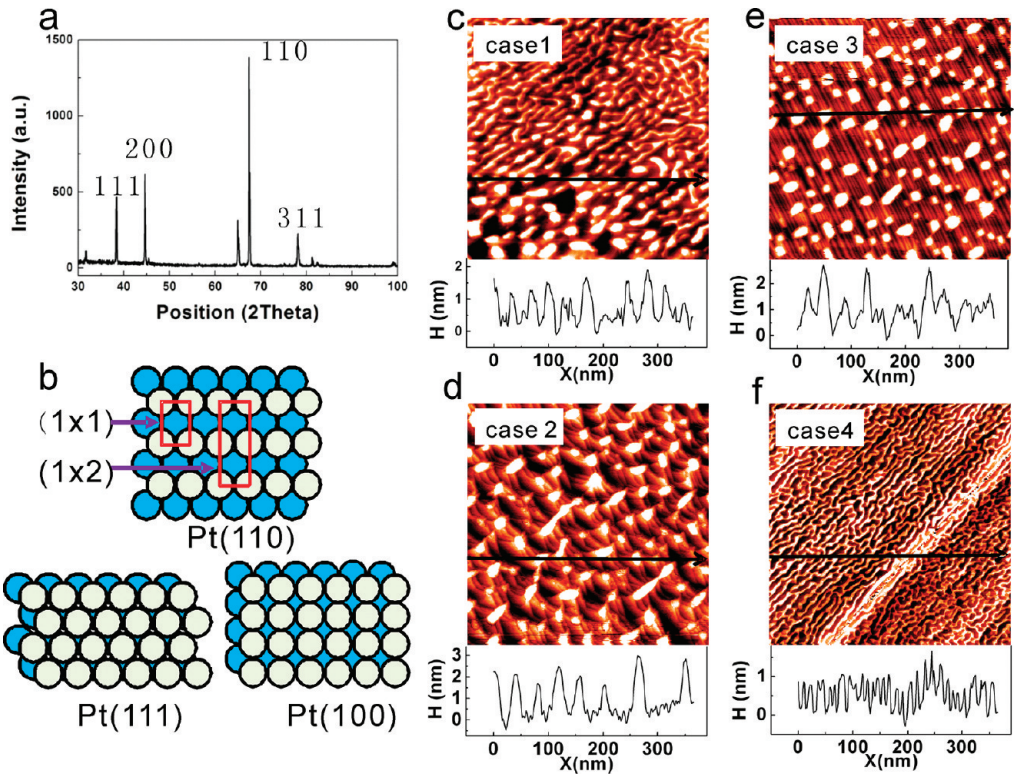

Figure 2. (a) XRD pattern of Pt foils after CVD growth. (b) Schemetic views showing the atomic models of various Pt facets. (c–f) Typical surface morphologies characterized with STM images and their height profiles (V_T = −0.15 V, I_T = 1.55 nA; −1.42 V, 1.06 nA; −1.54 V, 0.82 nA; −0.004 V, 3.25 nA) (370 nm × 370 nm). According to the main facets involved, they are named case 1, case 2, case 3, and case 4, respectively.

With reference to the continuity, the growth rate, as well as the atomic structure of graphene, atomically resolved STM images are then captured in equivalence to the four cases. In a small-scale image of Figure 3a, the surface labeled as case 1 is found to be mainly composed of darker striped islands and brighter individual islands of irregular shapes. Sequential zoom-in images at the boundary of both typical regions (Figure 3b,c) show perfect hexagonal lattices on the lower bright island and quadrate lattices on the upper striped island, and both lattices connect well at the boundary. Considering the lattice match effect, the facet underneath the hexagonal lattice is proposed to be Pt(111). According to published references, the formation of the stripped islands coincides well with a mesoscopic self-organization of Pt(110)-(1 × 2) induced by the intrinsic surface stress effect.[27] Hence, the dim quadrate lattice in the upper left corner of Figure 3c should be in line with the atomically resolved image of Pt(110)-(1 × 2), possibly along with a little contribution from the electronic state effect of graphene. In Figure 3d,e, another two atomically resolved images manifesting different island shapes are supplied for reconfirming the perfect continuity of hexagonal and quadrate lattices at the boundaries of various Pt facets.

It is fascinating to know if graphene exists over Pt(110)-(1 × 2) and whether the hexagonal lattice

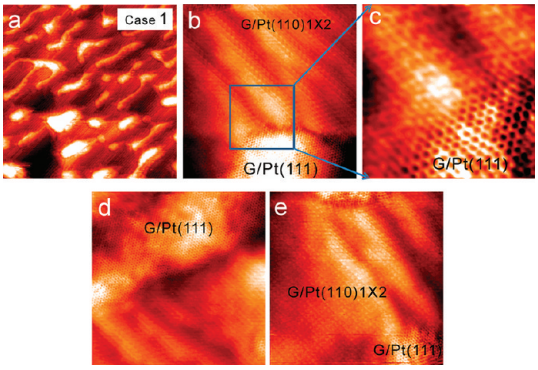

Figure 3. (a) Graphene formation on intermixing Pt(111) and Pt(110)-(1 × 2) regions imaged as brighter individual islands and darker striped patterns, respectively (V_T = −0.07 V, I_T = 1.55 nA; 150 nm × 150 nm). (b) V_T = −0.003 V, I_T = 1.74 nA; 15 nm × 15 nm and (c) V_T = −0.003 V, I_T = 1.74 nA; 4.4 nm × 4.4 nm) sequential zoom-in images showing a perfect continuity of graphene lattices over the two facets. (d) V_T = −0.12 V, I_T = 1.45 nA and (e) V_T = −0.003 V, I_T = 1.70 nA (15 nm × 15 nm) atomic-scale images of graphene over Pt(111) and Pt(110)-(1 × 2).

can be directly imaged or not. Figure 4a is an atomic-scale STM image with a tip change at the middle point, where quadrate lattices for Pt(110)-(1 × 2) and defect-free hexagonal lattices can be obtained in the lower and in the upper half of the image, respectively. After the tip change, repetitive scanning of the same area always displays hexagonal lattices on the whole

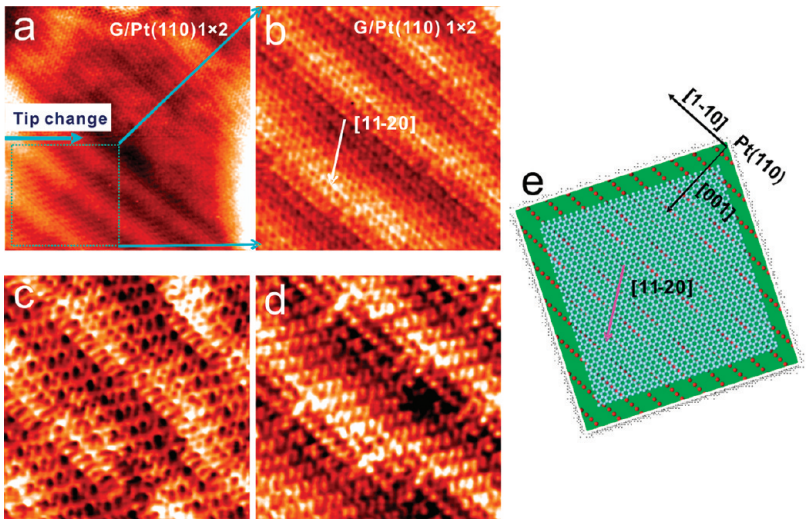

Figure 4. (a) Atomic-scale resolution image of graphene on Pt(110)-(1 × 2) with a tip change in the middle point, showing both Pt (lower part) and graphene (upper part) lattices (V_T = −0.003 V, I_T = 5.0 nA; 15 nm × 15 nm). (b) Hexagonal lattices obtained on the circled region of (a) right after the tip change (V_T = −0.003 V, I_T = 7.84 nA; 8.8 nm × 8.8 nm). (c,d) STM morphologies captured at the same location while under different tunneling conditions (−0.003 V, 7.8 nA; −0.002 V, 8.63 nA; 6 nm × 6 nm). (e) Schematic view of graphene growth on Pt(110)-(1 × 2).

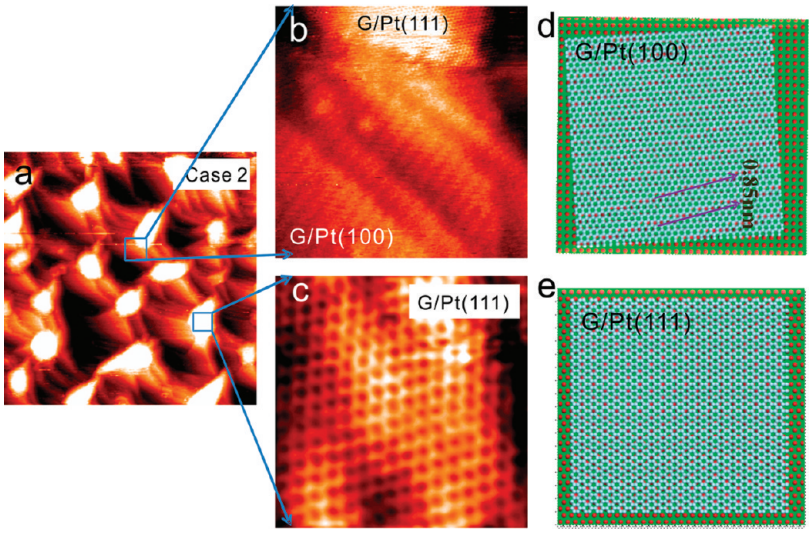

Figure 5. (a,b) STM images showing the perfect continuity of graphene lattices over interweaving Pt(111) and Pt(100) regions (V_T = −0.93 V, I_T = 2.75 nA; −0.002 V, 0.48 nA) (150 nm × 150 nm; 15 nm × 15 nm). The stripes in (b) are Moiré patterns having a distance of ∼0.85 nm. (c) Zoom-in image on Pt(111) showing hexagonal carbon lattices (V_T = −0.002 V, I_T = 0.48 nA; 3.7 nm × 3.7 nm). (d) Schematic illustration of the striped Moiré pattern formation by applying a 4° rotation of graphene lattice with respect to Pt(100). (e) Similar atomic model of graphene on Pt(111).

image. As an example, Figure 4b is captured on the lower square of Figure 4a, and the lattice constant analysis of the hexagonal lattice by STM section views provides a value of 0.246 nm. All of these results suggest that Pt(110)-(1 × 2) regions are definitely covered by monolayer graphene while the lattice may not be visible due to the strong substrate effect. Note that, in addition to this unexpected tip change effect, another significant finding is that the appearance and the disappearance of the graphene lattice depends strongly on tunneling conditions, as illustrated in Figure 4c,d, where even higher-resolution STM images are acquired under tunneling conditions of −0.003 V, 7.8 nA for Figure 4d and −0.003 V, 8.6 nA for Figure 4e.

Hereby, it can be deduced that strong modulations of Pt(110)-(1 × 2) lattices on graphene lattices indeed occur. This is understandable considering that the STM morphology is customarily a convolution of the morphology and the electronic structure of graphene and substrates. The graphene lattice and the substrate lattice can be imaged separately by STM under different tunneling conditions. A schematic illustration of this substrate effect is exhibited in Figure 4e. Of particular interest is that, with covering on small facets of Pt(111) and Pt(110)-(1 × 2),

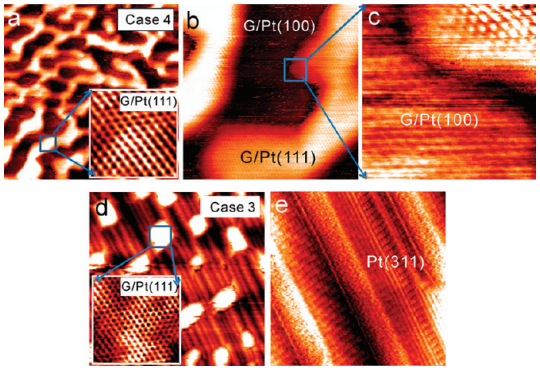

Figure 6. (a–c) STM morphologies showing the formation of continuous graphene over Pt surfaces composed of fractional islands and dark backgrounds (V_T = −0.032 V, I_T = 3.66 nA; −0.025 V, 4.72 nA; −0.003 V, 4.72 nA) (73 nm × 73 nm, 15 nm × 15 nm, 3.7 nm × 3.7 nm). The inset in (a) displays the observed hexagonal lattices on the island surface (V_T = −0.003 V, I_T = 29.8 nA; 2.4 nm × 2.4 nm). (d,e) Another typical surface consisting of striped Pt(311) and spot-like Pt(111) islands (V_T = −1.74 V, I_T = 0.72 nA; 150 nm × 150 nm; and V_T = −0.05 V, I_T = 1.46 nA; 24 nm × 24 nm). The inset in (d) again presents the formation of perfect monolayer graphene over small Pt(111) islands (V_T = −0.003 V, I_T = 29.8 nA; 3.7 nm × 3.7 nm). In contrary, the surrounding Pt(311) regions are almost free of graphene.

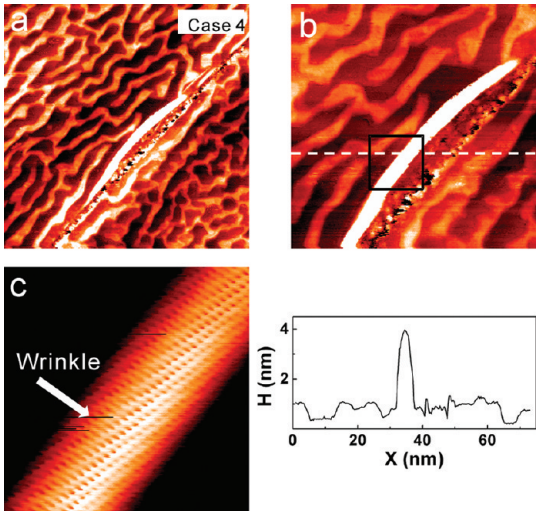

Figure 7. (a,b) STM images of a wrinkle-like structure (V_T = −0.04 V, I_T = 3.23 nA; 150 nm × 150 nm, 73 nm × 73 nm). Its section view along the line in (b) presents a height of ~3 nm over a lateral distance of ~7 nm. (c) Expanded image on the square in (b) showing twisted hexagonal lattices on the wrinkle surface (V_T = −0.04 V, I_T = 3.23 nA; 7.3 nm × 7.3 nm).

the CVD graphene is continuous and defect-free when examined at atomic scales, which, in turn, guarantees its two-dimensional (2D) growth at least up to micrometer scales.

In Figure 5, the surface typical for case 2 is exhibited which consists of the same high islands as that of case 1 and background triangular islands. Perfect hexagonal lattice again occurs on the individual bright islands of Pt(111) (Figure 5c), and a tentative model for the graphene growth is shown in Figure 5e. Of particular significance is that enlarged images over both typical regions in Figure 5b,c indicate a perfect extension of the carbon lattice from the high island of Pt(111) to the neighboring domains with the formation of striped superstructures. The spacing between the stripes is measured to be ~0.85 nm. By virtue of XRD data, the striped superstructure is proposed to originate from the relative rotation of graphene hexagonal lattice with respect to the square lattice of Pt(100).[10,12,21] A perfect simulation can be achieved by making a 4° rotation of the carbon lattice with respect to Pt(100), as schematically shown in Figure 5d.

STM morphologies displayed in Figure 6a–c and Figure 6d,e illustrate relative small-scale STM morphologies for case 4 and case 3, respectively. For case 4, the surface is observed to be made up of intermixing brighter fractional and darker flat regions, probably corresponding to Pt(111) and Pt(100) facets, respectively. The Pt(111) nature can be validated by the perfect hexagonal lattice obtained above, evidenced by an inset in Figure 6a. A perfect continuity of the graphene lattice can also be achieved even at the facet boundaries of Pt(111) and Pt(100) (Figure 6b,c). For case 3 in Figure 6d composed of striped Pt(311) and randomly distributed Pt(111) facets, perfect hexagonal lattices can be acquired in the inset of Figure 6d. In contrast, almost no atomic lattice appears on Pt(311) (Figure 6e). It is worthy to note that the preannealing treatment of Cu foils is essential through which the surface facets that are not suitable for graphene growth such as Pt(311) can be reduced dramatically. Accordingly, the uniformity and the continuity of the graphene films can be much improved.

On the basis of above systematic STM characterizations, it is deduced that the Pt substrate crystallography has a significant effect on graphene growth. Pt(111) is proposed to be the most suitable substrate toward high-quality graphene in terms of lattice symmetry match effect. Subsequently, Pt(100) and Pt(110) are the preferable substrates with the formation of striped superstructures and perfect hexagonal lattices, respectively. These surface features originate from the convolution of the electronic states and the lattice arrangements of graphene and metal substrates. Due to the huge lattice mismatch effect, graphene over Pt(311) shows the worst continuity compared to other low index facets.

Besides being multifaceted, other surface features that may alter the flatness and ultimately depress the quality of as-grown graphene are the ever-present wrinkles and ripples, which are usually proposed to evolve for releasing strains from the thermal expansion mismatch between graphene and substrates.[28,29] It is known that the thermal expansion coefficient of graphite varies from -1.25×10^{-6}/K at 20 °C to 1.25×10^{-6}/K at 1000 °C. However, the value for Pt changes from 8.8×10^{-6}/K to 11.96×10^{-6}/K at the same temperature range,

which is much smaller than that of Cu.[26] As a result, the net uniaxial contraction ($\Delta L/L_{293}$) of Pt at 1300 K equals 1.03% in comparison with Cu of 1.8%. This difference is well reflected by large-scale STM examinations which present fewer wrinkles on Pt foils than that on Cu foils. Shown in Figure 7b is a striped structure, and its section view illustrates a height fluctuation of ~3 nm over a lateral distance of ~7 nm, in parallel with the dimension of wrinkles. An atomically resolved image on the wrinkle surface (Figure 7c) demonstrates twisted hexagonal lattices, again corresponding well with the characteristics of folded graphene.

In addition to the formation of wrinkles, the conformation of two-dimensional (2D) graphene lattice to the undulated Pt foil substrate is expected to contribute another pathway for stress relief, as similarly reported for graphene growth on Ru(0001) where a Moiré structure is formed along with obvious surface corrugations.[30] Why is this pathway proposed? As mentioned above, the Pt foils after CVD growth are ordinarily textured with Pt(110), Pt(100), and Pt(111) facets having an average dimension of several tens of square nanometers, which is much smaller than that of Cu foils.[26] Meanwhile, the the Pt surface after CVD growth usually manifests a roughness of ~2 nm over several hundred nanometers, indicating a more flat surface than that of Cu foils. In this case, through graphene's conformation to the substrate undulations, extra strains arising from the thermal expansion mismatch can be released on the undulated Pt foils. Accordingly, the density of pristine wrinkles is much reduced.

CONCLUSION

Using an ambient pressure CVD method, we accomplished the synthesis of high-quality monolayer graphene on Pt foils and characterized its single-layer nature using Raman spectroscopy in combination with SEM. The growth of monolayer graphene on Pt foils is proposed to be directed by a surface-catalyzed growth mechanism. The perfect continuity of CVD graphene on Pt foils was then examined using atomically resolved STM. We find that monolayer graphene grows mainly in registry with the symmetries of the underlying Pt facets with the formation of hexagonal lattices and striped superstructures, and strangely, they can be connected well at the facet boundaries. Moreover, we investigate the substrate crystallography effects on the growth of graphene, where Pt(111) and Pt(100) facets are detected to be more preferred than other low-index facets to serve as the growth substrates. In addition, we report that graphene on Pt foils presents more flat surfaces than that on Cu foils, which implies the formation of extra high-quality graphene even at the as-grown state. As a result, we believe that graphene on Pt foils provides a perfect prototype for exploring the preliminary growth dynamics of CVD processes.

METHODS

Preparation of Graphene. Graphene was prepared according to a literature procedure.[16] Briefly, Pt foils with a thickness of 25 μm were used as substrates for graphene growth inside a quartz tube furnace. The furnace was first flowed with 50 sccm H_2 and 850 sccm Ar gas for 15 min while the temperature was increased from room temperature to 1050 °C. Then, 10 sccm CH_4 was introduced into the furnace at 1050 °C for 12 min for cracking CH_4. Finally, the sample was cooled to room temperature with a cooling rate of 20 °C/min. The thicknesses of graphene samples can be controlled by varying the growth time or increasing the growth temperature.

SEM, Raman, and STM Characterizations. The macroscopic morphology and the thickness of CVD graphene prior to the chemical etching transfer were characterized with SEM and Raman spectroscopy. To achieve atomically resolved images, the as-grown samples were transferred into an Omicron ultrahigh vacuum variable-temperature scanning tunneling microscopy (UHV-VT-STM), annealed for several hours to remove the adsorbed impurities, and then examined by STM working at a constant current mode with the sample kept at room temperature. The graphene sample was also transferred to a 300 nm thick SiO_2/Si substrate by wet chemical etching the metal support using dilute aqua regia solution. The transferred graphene was then characterized with an optical microscope and Raman spectroscopy to show its two-dimensional homogeneity and thickness.

Acknowledgment. This work was financially supported by the National Natural Science Foundation of China (Grant Nos. 21073003, 20973006, 20973013, 51072004, 50821061, 20833001) and The Ministry of Science and Technology of China (Grant Nos. 2011CB921903, 2011CB933003, 2012CB921404).

REFERENCES AND NOTES

1. Geim, A. K.; Novoselov, K. S. The Rise of Graphene. *Nat. Mater.* **2007**, *6*, 183–191.
2. Castro Neto, A. H.; Guinea, F.; Peres, N. M.; Novoselov, K. S.; Geim, A. K. The Electronic Properties of Graphene. *Rev. Mod. Phys.* **2009**, *81*, 109–162.
3. Novoselov, K. S.; Geim, A. K.; Morozov, S. V.; Jiang, D.; Zhang, Y.; Dubonos, S. V.; Grigorieva, I. V.; Firsov, A. A. Electric Field Effect in Atomically Thin Carbon Films. *Science* **2004**, *306*, 666–669.
4. Novoselov, K. S.; Geim, A. K.; Morozov, S. V.; Jiang, D.; Katsnelson, M. I.; Grigorieva, I. V.; Dubonos, S. V.; Firsov, A. A. Two-Dimensional Gas of Massless Dirac Fermions in Graphene. *Nature* **2005**, *438*, 197–200.
5. Zhang, Y. B.; Tan, Y. W.; Stormer, H. L.; Kim, P. Experimental Observation of the Quantum Hall Effect and Berry's Phase in Graphene. *Nature* **2005**, *438*, 201–204.
6. Li, X. S.; Zhu, Y.; Cai, W. W.; Borysiak, M.; Han, B.; Chen, D.; Piner, R. D.; Colombo, L.; Ruoff, R. S. Transfer of Large-Area Graphene Films for High-Performance Transparent Conductive Electrodes. *Nano Lett.* **2009**, *9*, 4359–4363.
7. Li, X. S.; Cai, W. W.; An, J. H.; Kim, S.; Nah, J.; Yang, D. X.; Piner, R. D.; Velamakanni, A.; Jung, I.; Tutuc, E.; *et al.* Large-Area Synthesis of High-Quality and Uniform Graphene Films on Copper Foils. *Science* **2009**, *324*, 1312–1314.

8. Li, X. S.; Cai, W. W.; Colombo, L.; Ruoff, R. S. Evolution of Graphene Growth on Cu and Ni Studied by Carbon Isotope Labeling. *Nano Lett.* **2009**, *9*, 4268–4272.
9. Huang, P. Y.; Ruiz-Vargas, C. S.; van der Zande, A. M.; Whitney, W. S.; Levendorf, M. P.; Kevek, J. W.; Garg, S.; Alden, J. S.; Hustedt, C. J.; Zhu, Y.; *et al.* Grains and Grain Boundaries in Single-Layer Graphene Atomic Patchwork Quilts. *Nature* **2011**, *469*, 389–392.
10. Zhao, L.; Rim, K. T.; Zhou, H.; He, R.; Heinz, T. F.; Pinczuk, A.; Flynn, G. W.; Pasupathy, A. N. Influence of Copper Crystal Surface on the CVD Growth of Large Area Monolayer Graphene. *Solid State Commun.* **2011**, *151*, 509–513.
11. Gao, L.; Guest, J. R.; Guisinger, N. P. Epitaxial Graphene on Cu(111). *Nano Lett.* **2010**, *10*, 3512–3516.
12. Rasool, H. I.; Song, E. B.; Alle, M. J.; Wassei, J. K.; Kaner, R. B.; Wang, K. L.; Weiller, B. H.; Gimzewski, J. K. Continuity of Graphene on Polycrystalline Copper. *Nano Lett.* **2011**, *11*, 251–256.
13. Wood, J. D.; Schmucker, S. W.; Lyons, A. S.; Pop, E.; Lyding, J. W. Effects of Polycrystalline Cu Substrate on Graphene Growth by Chemical Vapor Deposition. *Nano Lett.* **2011**, 10.1021/nl201566c.
14. Gao, M.; Pan, Y.; Huang, L.; Hu, H.; Zhang, L. Z.; Guo, H. M.; Du, S. X.; Gao, H.-J. Epitaxial Growth and Structural Property of Graphene on Pt(111). *Appl. Phys. Lett.* **2011**, *98*, 033101(1−3).
15. Otero, G.; González, C.; Pinardi, A. L.; Merino, P.; Gardonio, S.; Lizzit, S.; Blanco-Rey, M.; Van de Ruit, K.; Flipse, C. F.; Méndez, J.; *et al.* Ordered Vacancy Network Induced by the Growth of Epitaxial Graphene on Pt(111). *Phys. Rev. Lett.* **2010**, *105*, 216102(1−4).
16. Kang, B. J.; Mun, J. H.; Hwang, C. Y.; Cho, B. J. Monolayer Graphene Growth on Sputtered Thin Film Platinum. *J. Appl. Phys.* **2009**, *106*, 104309(1−6).
17. Yu, Q. K.; Jauregui, L. A.; Wu, W.; Colby, R.; Tian, J. F.; Su, Z. H.; Gao, H. L.; Liu, Z. H.; Pandey, D.; Wei, D. G.; *et al.* Control and Characterization of Individual Grains and Grain Boundaries in Graphene Grown by Chemical Vapour Deposition. *Nat. Mater.* **2011**, *10*, 443–449.
18. Robertson, A. W.; Warner, J. H. Hexagonal Single Crystal Domains of Few-Layer Graphene on Copper Foils. *Nano Lett.* **2011**, *11*, 1182–1189.
19. Lee, S. H.; Lee, K. H.; Zhong, Z. H. Wafer Scale Homogeneous Bilayer Graphene Films by Chemical Vapor Deposition. *Nano Lett.* **2010**, *10*, 4702–4707.
20. Yan, K.; Peng, H. L.; Zhou, Y.; Li, H.; Liu, Z. F. Formation of Bilayer Bernal Graphene: Layer-by-Layer Epitaxy *via* Chemical Vapor Deposition. *Nano Lett.* **2011**, *11*, 1106–1110.
21. Rasool, H. I.; Song, E. B.; Mecklenburg, M.; Regan, B. C.; Wang, K. L.; Weiller, B. H.; Gimzewski, J. K. Atomic-Scale Characterization of Graphene Grown on Copper (100) Single Crystals. *J. Am. Chem. Soc.* **2011**, *133*, 12536–12543.
22. Ferrari, A. C.; Meyer, J. C.; Scardaci, V.; Casiraghi, C.; Lazzeri, M.; Mauri, F.; Piscanec, S.; Jiang, D.; Novoselov, K. S.; Roth, S.; *et al.* Raman Spectrum of Graphene and Graphene Layers. *Phys. Rev. Lett.* **2006**, *97*, 187401(1−4).
23. Hao, Y. F.; Wang, Y. Y.; Wang, L.; Ni, Z. H.; Wang, Z. Q.; Wang, R.; Koo, C. K.; Shen, Z. X.; Thong, J. T. L. Probing Layer Number and Stacking Order of Few-Layer Graphene by Raman Spectroscopy. *Small* **2010**, *6*, 195–200.
24. Liu, N.; Fu, L.; Dai, B. Y.; Yan, K.; Liu, X.; Zhao, R. Q.; Zhang, Y. F.; Liu, Z. F. Universal Segregation Growth Approach to Wafer-Size Graphene from Non-Noble Metals. *Nano Lett.* **2011**, *11*, 297–303.
25. Isett, L. C.; Blakely, J. M. Segregation Isosteres for Carbon at the (100) Surface of Nickel. *Surf. Sci.* **1976**, *58*, 397–414.
26. Zhang, Y. F.; Gao, T.; Gao, Y. B.; Xie, S. B.; Ji, Q. Q.; Yan, K.; Peng, H. L.; Liu, Z. F. Defect-like Structures of Graphene on Copper Foils for Strain Relief Investigated by High-Resolution Scanning Tunneling Microscopy. *ACS Nano* **2011**, *5*, 4014–4022.
27. Hanesch, P.; Bertel, E. Mesoscopic Self-Organization Induced by Intrinsic Surface Stress on Pt(110). *Phys. Rev. Lett.* **1997**, *79*, 1523–1526.
28. Spiecker, E.; Schmid, A. K.; Minor, A. M.; Dahmen, U.; Hollensteiner, S.; Jäger, W. Self-Assembled Formation of Nanofold Networks on Layered Crystal Surfaces during Metal Intercalation. *Phys. Rev. Lett.* **2006**, *96*, 086401(1−4).
29. Chae, S. J.; Gunes, F.; Kim, K. K.; Kim, E. S.; Han, G. H.; Kim, S. M.; Shin, H. J.; Yoon, S. M.; Choi, J. Y.; Park, M. H.; *et al.* Synthesis of Large-Area Graphene Layers on Poly-nickel Substrate by Chemical Vapor Deposition: Wrinkle Formation. *Adv. Mater.* **2009**, *21*, 2328–2333.
30. Vázquez de Parga, A. L.; Calleja, F.; Borca, B.; Passeggi, M. C. G.; Hinarejos, J. J.; Guinea, F.; Miranda, R. Periodically Rippled Graphene: Growth and Spatially Resolved Electronic Structure. *Phys. Rev. Lett.* **2008**, *100*, 056807(1−4).